Temporal characteristics of functional connectome reconfigurations are heritable and related to cognition.

Suhnyoung Jun[1,2], Thomas H. Alderson[1], Andre Altmann[3], Sepideh Sadaghiani[1,2,4]*

[1] Beckman Institute for Advanced Science and Technology, University of Illinois at Urbana-Champaign, Urbana, Illinois, 618201
[2] Psychology Department, University of Illinois at Urbana-Champaign, Urbana, Illinois 61801
[3] Centre for Medical Image Computing (CMIC), Department of Medical Physics, University College London, London, UK
[4] Neuroscience Program, University of Illinois at Urbana-Champaign, Urbana, Illinois 61801

***Correspondence**: Sepideh Sadaghiani
Email: sepideh@illinois.edu

Author Contributions: SJ and SS designed research; SJ performed research; SJ analyzed data; SJ and SS wrote the paper; and SS, THA and AA contributed analytic expertise, theoretical guidance, paper revisions, and informed interpretation of the results.

Keywords: dynamic functional connectivity; heritability; variance component modeling; twin study, hidden Markov modelling.

This PDF file includes:

Main Text
Figures 1 to 4
Table 1

Abstract

The brain's functional connectivity architecture (functional connectome) is dynamic, constantly reconfiguring in an individual-specific manner and contributing to inter-individual variability in cognitive performances. However, to what extent genetic effects shape the dynamic reconfigurations of the functional connectome is largely unknown. This paper assesses whether dynamic connectome features are heritable, quantifies their heritability, and explores their association with cognitive phenotypes. We identified discrete connectome states from resting-state fMRI data (n = 1003 including twins and non-twin siblings) and obtained multivariate features, each describing temporal or spatial characteristics of connectome dynamics. We found strong evidence that the temporal features, particularly fractional occupancy (FO) and transition probability (TP), were heritable. Importantly, a substantial proportion of phenotypic variance of these features (35% of FO and 41% of TP) was explained by genetic effects. The effect was stable after adjusting for head motion, independent of global signal regression and the chosen number of states, and absent in surrogate data. Contrarily, the data did not provide robust support for heritability of spatial features suggesting that genetic effects primarily contribute to how the connectome *transitions* across states, rather than the precise way in which the states are spatially instantiated. Notably, temporal phenotypes also captured variability in cognitive performance. Overall, our findings demonstrate a link between genetic makeup and temporal reconfigurations of the functional connectome, suggesting that dynamic features may act as endophenotypes for cognitive abilities. In conclusion, we propose that connectome dynamics offer considerable potential as a theoretical, conceptual, and practical framework for linking genetics to behavior.

Introduction

Inter-individual variability in the time-averaged (static) functional connectivity architecture of the human brain is subject-specific and predictive of cognitive abilities (1–4). With the increasing availability of large-sample fMRI datasets, significant genetic contributions to this static large-scale connectome architecture have been established. Specifically, the heritability of individual edge-wise connections and networks of the functional connectome has been identified (5, 6). Moreover, topological properties of the static connectome, such as the modular organization, constitute heritable subject-specific traits and are linked to behavioral and cognitive traits (7, 8).

However, the static architecture captures only part of the functionally significant properties of the connectome. In fact, the functional connectome as measured by fMRI exhibits flexible reconfigurations over the course of seconds to minutes (9, 10). These reconfigurations can be described as changes in connectivity strength between specific sets of brain region-pairs, forming recurrent connectome states. Such functional connectome states hold great significance as their time-varying (dynamic) characteristics have been linked to behavior and cognition as detailed below (11, 12).

Because some of the same behavioral and cognitive features linked to connectome dynamics are also heritable (13), the exciting possibility emerges that the behaviorally relevant connectome dynamics may themselves have heritable characteristics. A fundamental question is which specific features of the functional connectome dynamics may be heritable. Especially in light of the virtually unlimited number of properties that characterize connectome dynamics, we argue that the focus should be on features that are of behavioral significance.

In particular, specific dynamic changes in *spatial* features of the connectome shape behavior. An often reported observation is that variability of functional connectivity (FC) between the default-mode network (DMN) and top-down control regions affect behavioral outcomes (14, 15). Most notably, FC dynamics between the DMN and the frontoparietal network (FPN) have been linked to cognitive flexibility (16–18). Spatial connectome patterns can further be succinctly quantified as global topological properties of the connectome's graph representation. A critical topological property is Modularity, which quantifies the balance between segregation (prioritizing processing within specialized networks) and integration (combining specialized information from various networks) (19). Modularity is the topological feature commonly associated with various behavioral outcomes (14, 20–23).

Beyond these spatial features, specific *temporal* features of connectome dynamics have been very fruitful in the context of behavioral relevance (24). Specifically, the proportion of the total recording time spent in each connectome state (fractional occupancy, or FO) and the probability to transition between specific pairs of discrete states (transition probability, or TP) have been linked

to behavior (11, 12). Moreover, the time spent in two "metastates", identified from hierarchical clustering of FO over fine-grained states, was found to be heritable (12). Temporal features are of particular interest to the current study of connectome dynamics as they characterize the *trajectory* of the connectome across state space rather than the states per se.

Based on the above-described prior work establishing behaviorally consequential features of connectome dynamics, we chose to investigate two spatial and two temporal features: (1) FC between DMN and FPN ($FC_{DMN\text{-}FPN}$); (2) Modularity; (3) FO; and (4) TP between states. Focusing on these features, we sought to answer (i) whether spatial and topological features of discrete connectome states are heritable; (ii) whether temporal features characterizing the spontaneous reorganization across these states are heritable; (iii) whether dynamic connectome features are inherited as individual traits or collectively as multivariate features; (iv) how much of the individual phenotypic differences can be accounted for by genetic influence; and (v) how inter-individual variability in such dynamic features contributes to differences in cognitive abilities. To answer these questions, we studied resting-state fMRI data from the Human Connectome Project, including monozygotic and dizygotic twin pairs, non-twin sibling pairs, and pairs of unrelated individuals. We extracted discrete brain states, estimated their dynamic features, fitted quantitative genetic models to the features, and quantified their association with cognition.

Results

Fig. 1 illustrates the overall approach and analyses performed for each subsection of the Results.

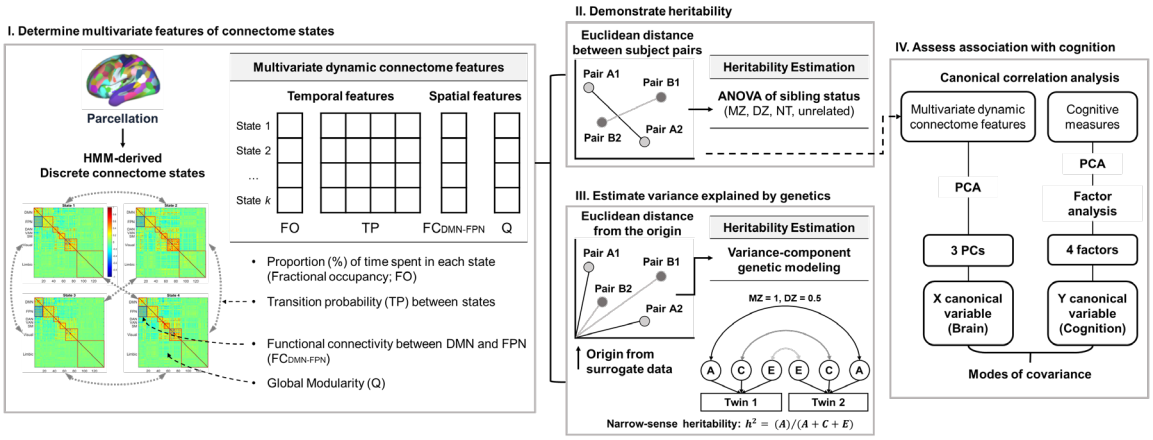

Fig. 1. An overview of the method pipeline. We used minimally preprocessed resting state BOLD timeseries from 139 group-ICA-derived regions covering cortical and subcortical areas of the

cerebrum as provided by the Human Connectome Project. [Section I] We applied a hidden Markov modeling (HMM) approach to extract four discrete connectome states (or six states for replication, respectively). Four multivariate features describing the connectome dynamics were obtained at the subject level. Multivariate temporal features were defined as the proportion of the total recording time spent in each connectome state (fractional occupancy, or FO) and the probability matrix of transitioning between every pair of discrete states (transition probability, or TP). Multivariate spatial features were defined as the functional connectivity between default mode and frontoparietal networks ($FC_{DMN\text{-}FPN}$) and global modularity (Q). All state-specific features (i.e., FO, $FC_{DMN\text{-}FPN}$, and Q) differed significantly across states. [Section II] We tested whether genetically related subjects had more similar multivariate features than genetically less related subjects. The similarity of each feature between a given pair of subjects was quantified as Euclidean distance. Distance values entered a one-way ANOVA of the factor sibling status with the four levels of monozygotic twins (MZ; 120 pairs), dizygotic twins (DZ; same-sex 65 pairs), non-twin siblings (NT; 169 pairs), and pairs of unrelated individuals (88 pairs). [Section III] To estimate the heritability and quantify the genetic effects, we employed the structural equation model (i.e., genetic variance component model) to partition the phenotypic variance of a trait into additive genetic (denoted A), common environmental (denoted C) and unique environmental components (denoted E), where a narrow-sense heritability (h^2) is quantified as the proportion of variance attributed to the genetic factor (A). Particularly, the path A depends on the genetic similarity between twins: whereas MZ twins are genetically identical (path denoted MZ = 1), DZ twins share half of their genetic information (path denoted DZ = 0.5) based on the supposition of Mendelian inheritance. To accommodate our multivariate features in the model, we computed the distance between the position of the feature and a null model-derived tangent point in multivariate space. [Section IV] Canonical correlation analysis was used to find modes of population covariation between multivariate dynamic connectome features and cognition. This analysis was performed on dimensionality reduced connectome features (three components from principal component analysis (PCA)) and behavioral data (four factors from factor analysis).

I. Discrete connectome states have distinct spatial and temporal features

We applied a hidden Markov modeling (HMM) approach to extract four discrete connectome states, i.e., whole-brain connectivity patterns that repeatedly appear at different time points, in a data-driven fashion (Fig. 2) (25). Since HMMs require an *a priori* selection of the number of states (*K*), we chose two values of *K* within the range of prior HMM literature (*K* = 3 to 12 (12, 25–31)) with the reasoning that robust heritability effects should be observable for both *K*s (cf. Me thods). We report outcomes for *K* = 4 in the following and provide replicated results of *K* = 6 in *SI Appendix*.

We performed a one-way ANOVA (factor state) of the connectome states' temporal and spatial features of interest to assess whether the HMM has successfully inferred states with distinguishable network organization. Specifically, we tested the strength of FC between DMN and FPN ($FC_{DMN\text{-}FPN}$), the degree of global modular organization (Newman's Modularity (32)), and the proportion of time spent in each state, that is, Fractional Occupancy (FO).

Fig. 2 shows that the connectome states differed with respect to $FC_{DMN\text{-}FPN}$ ($F_{(3,\ 3976)}$ = 399.41 with P = 1.18e-217), Modularity ($F_{(3,\ 3717)}$ = 189.65 with P = 1.96e-114), and FO ($F_{(3,\ 3996)}$ = 105.00 with P = 1.98e-65). Regarding temporal characteristics, the distribution of FO over the states as well as the TP between states were not random (tested for the four- and six-state models against surrogate data, *SI Appendix, Fig. S10*). These results show that the spontaneous connectivity time course can be described as a (non-random) sequence of four (respectively six) connectome states, differing from each other in spatial organization and global topology.

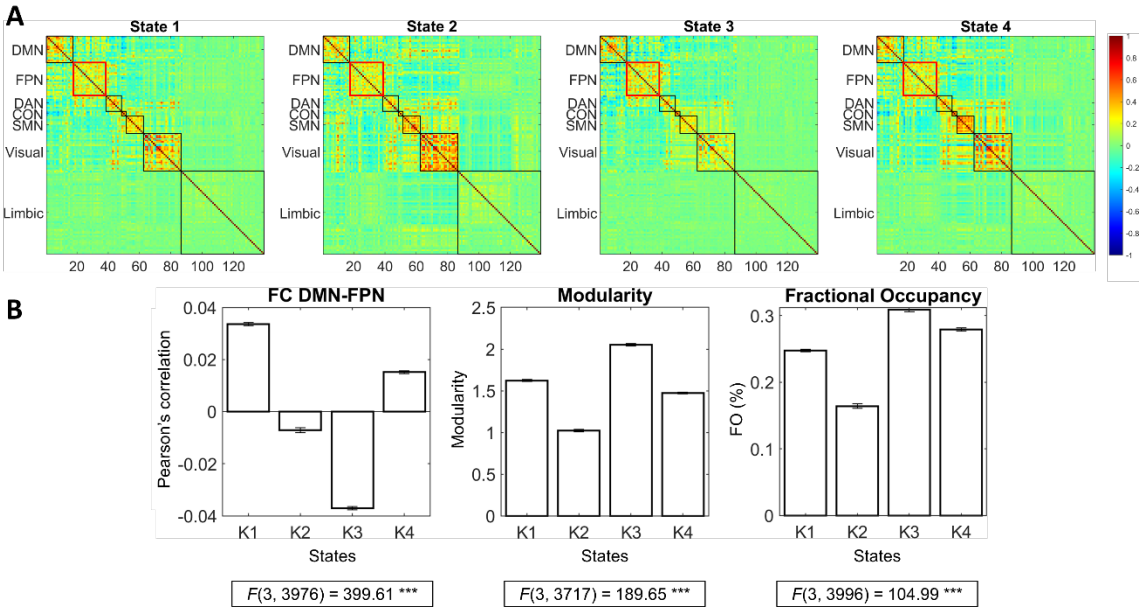

Fig. 2. HMM-inferred connectome states. (A) Group-level functional correlation matrices based on 139 regions covering cortical and subcortical areas of the cerebrum for four HMM-derived states. The rows and columns represent regions and are organized according to the corresponding ICNs (visual network (VIS), sensory-motor network (SMN), dorsal attention network (DAN), salience/cingulo-opercular network (CON), limbic network (Limbic), frontoparietal network (FPN), and default mode network (DMN)). Each element of the matrix is a z-scored Pearson's correlation coefficient representing the functional connection between the corresponding regions. (B) Bar plots

of the mean of $FC_{DMN\text{-}FPN}$, Modularity, and FO for each state from all 1003 subjects. *F* values are reported for one-way ANOVAs of the factor state for each variable. *** indicates $p < 10^{-60}$.

II. Multivariate temporal features of the dynamic connectome are heritable.

All state-specific features that differed significantly across states in the above-described analysis ($FC_{DMN\text{-}FPN,}$ Modularity, and FO), as well as TP between these states, were then tested for heritability. We treated the 1 × *K* vectors of $FC_{DMN\text{-}FPN,}$ Modularity, FO, and *K* × *K* matrix of TP as *multivariate* features. To avoid statistical pitfalls of multiple comparisons, we limited heritability analyses to this hypothesis-driven selection of phenotypes (with additional exploratory analyses detailed below).

We tested whether genetically related subjects had more similar multivariate features than genetically less related subjects. The similarity of each multivariate connectome feature between a given pair of subjects was quantified as Euclidean distance (**Materials and Methods** – Comparison of multivariate features). Distance values entered a one-way ANOVA of the factor sibling status with the four levels of monozygotic (MZ) twins, same-sex dizygotic (DZ) twins, non-twin (NT) siblings, and pairs of unrelated individuals. Note that all pairs are uniquely defined so that none of the subjects overlap between groups.

Fig. 3A shows the heritability of temporal features of the connectome dynamics. Specifically, multivariate FO ($F_{(3, 438)}$ = 22.65, *P* = 1.19e-13) and TP ($F_{(3, 438)}$ = 17.91, *P* = 5.57e-11) phenotypes were more similar among MZ twins than DZ twins, followed by NT siblings and pairs of unrelated individuals. The effect of sibling status on multivariate dynamic connectome features was stable after adjusting for head motion parameters and independent of GSR and the chosen number of states (see *SI Appendix* – *Independence of heritability from parameter choices*, *Fig. S2*). Further, no effect of sibling status was observed in surrogate data with preserved static cross-covariance structure; FO ($F_{(3, 438)}$ = 1.30, *P* = .27) and TP ($F_{(3, 438)}$ = 1.14, *P* = .33).

Contrary to the temporal features, we did not find robust evidence for the heritability of multivariate spatial features. In particular, outcomes of equivalent ANOVAs for $FC_{DMN\text{-}FPN}$ ($F_{(3, 438)}$ = 3.40, *P* = 0.018) and Modularity ($F_{(3, 438)}$ = 3.47, *P* = 0.016) were small in effect size and dependent on the chosen number of states and global signal regression (*SI Appendix* – *Independence of heritability from parameter choices*, *Fig. S3*). The lack of heritability was confirmed by variance-component genetic analysis (see section III.).

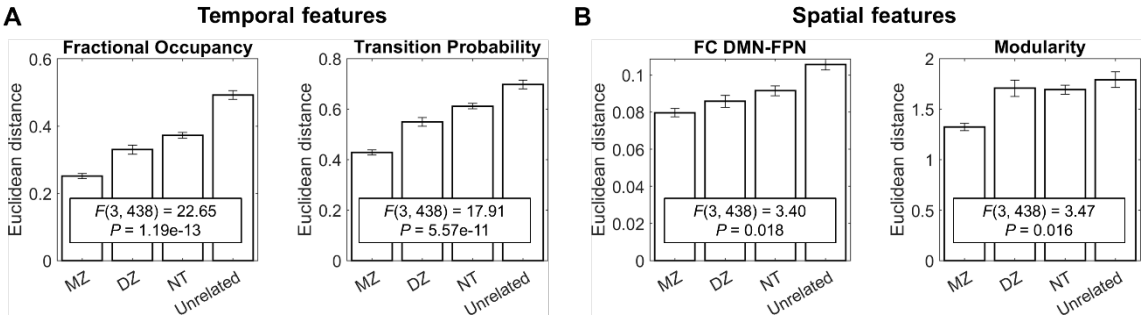

Fig. 3. Heritability of multivariate dynamic connectome features. To assess heritability, we compared the multivariate features across monozygotic twins (MZ; 120 pairs), dizygotic twins (DZ; 65 pairs), non-twin siblings (NT; 169 pairs), and pairs of unrelated individuals (88 pairs). *F* values are reported for one-way ANOVAs of the factor sibling status (four levels). A) Temporal connectome features, specifically the multivariate FO and TP phenotypes, were more similar among MZ twin pairs than DZ twins, followed by NT siblings and pairs of unrelated individuals. This influence of sibling status on multivariate dynamic connectome features as reflected in strong statistical outcomes was stable irrespective of GSR and the chosen number of states. B) On the other hand, for the spatial connectome features $FC_{DMN\text{-}FPN}$ and Modularity, evidence for heritability was not robust. Despite weakly significant difference across sibling groups in the four-state model visualized here, the pattern in the six-state model was incompatible with expectations of a heritable phenotype (cf. *Fig. S4*). Similarly, despite weakly significant differences in Modularity found here in the four-state model, the effect was absent in the six-state model (see *Fig. S4*).

To ensure that the lack of robust outcomes for spatial features was not driven by a narrow choice of such features, we further performed exploratory ANOVAs to assess the heritability of FC between DMN and the two other major top-down control networks (*SI Appendix – Exploring heritability of DMN connectivity to other networks*, *Fig. S4*), as well as a data-driven selection of edges (*SI Appendix – Exploring heritability with network-based statistics*, *Fig. S5*). Again, ANOVA outcomes were either dependent on the number of states and GSR or inconsistent with expectations in that DZ twins showed less similarity than NT siblings, suggesting that these spatial features may not be heritable. Potential reasons for such inconsistencies are discussed in the *SI Appendix*.

Interestingly, the *individual* components of multivariate features were not heritable (*Fig. S7*); that is, none of the state-wise dynamic connectome phenotypes differed by sibling status (i.e., no heritability effect), even though they showed clear differences across connectome states (See *Fig. S6* for the main effect of connectome states, in line with results of Fig. 2B). Therefore, the findings demonstrate that the temporal features of the dynamic connectome are heritable,

regardless of the spatial features of the connectome states, only as multivariate patterns encompassing all states, not as individual state-specific components.

III. Heritability accounts for substantial variance in multivariate dynamic connectome features across individuals.

We employed a structural equation modeling (33) to estimate the extent to which inter-individual differences in a phenotype are driven by genetic or environmental factors. The classical genetic variance component modeling quantifies the contribution of genetic factors to univariate phenotypes. However, our above-described ANOVAs suggest that temporal characteristics of connectome dynamics are inherited as multivariate phenotypes (Fig. 3A) rather than individual components (*Fig. S7*). We, therefore, adjusted the variance component modeling of univariate features to accommodate multivariate phenotypes by focusing on the position of the feature in multivariate space (cf. Fig. 1). For converging results from an alternative approach (34) for multivariate features, which, however, does not account for collinearities among the univariate components, see *SI Appendix* – *Alternative multivariate genetic variance component model*.

The ACE model showed that a substantial portion of variance of multivariate temporal dynamic connectome features was explained by the genetic effect (Table 1). The additive genetic effect (A) of FO was estimated as .35, resulting in a narrow-sense heritability of h^2 = .35 (i.e., accounting for 35% of the total phenotypic variance). The additive genetic effect of TP was estimated as .41, resulting in a narrow-sense heritability of h^2 =.41, again accounting for a substantial proportion of inter-individual variance in this measure. Note that the impact of common environment (C) was estimated as zero for both FO and TP. For both of these features, the fitness of the nested models was not significantly better than the full ACE model. We interpret these outcomes to suggest the involvement of substantial genetic contributions to the temporal features of connectome dynamics.

Contrary to the temporal features, the variance component modeling of the spatial features, $FC_{DMN\text{-}FPN}$ and Modularity, did not support a genetic effect. The h^2 of $FC_{DMN\text{-}FPN}$ was .21, but with a wide 95% confidence interval crossing zero ([-0.30, 0.72]). No heritability was found for Modularity (h^2=0). This confirms the lack of robust heritability effect observed from the ANOVA (Fig. 3 and *Fig. S3*) for $FC_{DMN\text{-}FPN}$ and Modularity.

IV. Temporal phenotypes of the dynamic connectome are associated with cognition

Finally, canonical correlation analysis (CCA) was used to relate the cognitive measures to temporal phenotypes of the dynamic connectome. The CCA, performed on three principal components of dynamic connectome phenotypes and four factors of cognitive measures, revealed

three modes of covariation (Fig. 4A). All modes were highly significant (against 10,000 permutations, $p < 10^{-4}$ (Fig. 4B-D)) and robust after correcting for FD head motion parameter. We used post-hoc correlations between the discovered modes and the cognitive factors to evaluate the contribution of each factor to each mode, with respect to the temporal phenotypes of the dynamic connectome. The first mode with the highest significance was defined by negative weights for the "Language" (r = -.18) and "Memory" (r = -.16) factors, followed by "Impulsivity" (r = -.12) and "Cognitive control" (r = -.10) (Fig. 4E). The second mode was defined by a positive weight for "Cognitive control" (r = .08) (Fig. 4F). The third mode was not defined by any specific cognitive factors (Fig. 4G). These results indicate that temporal phenotypes of the dynamic connectome are related to cognitive performance.

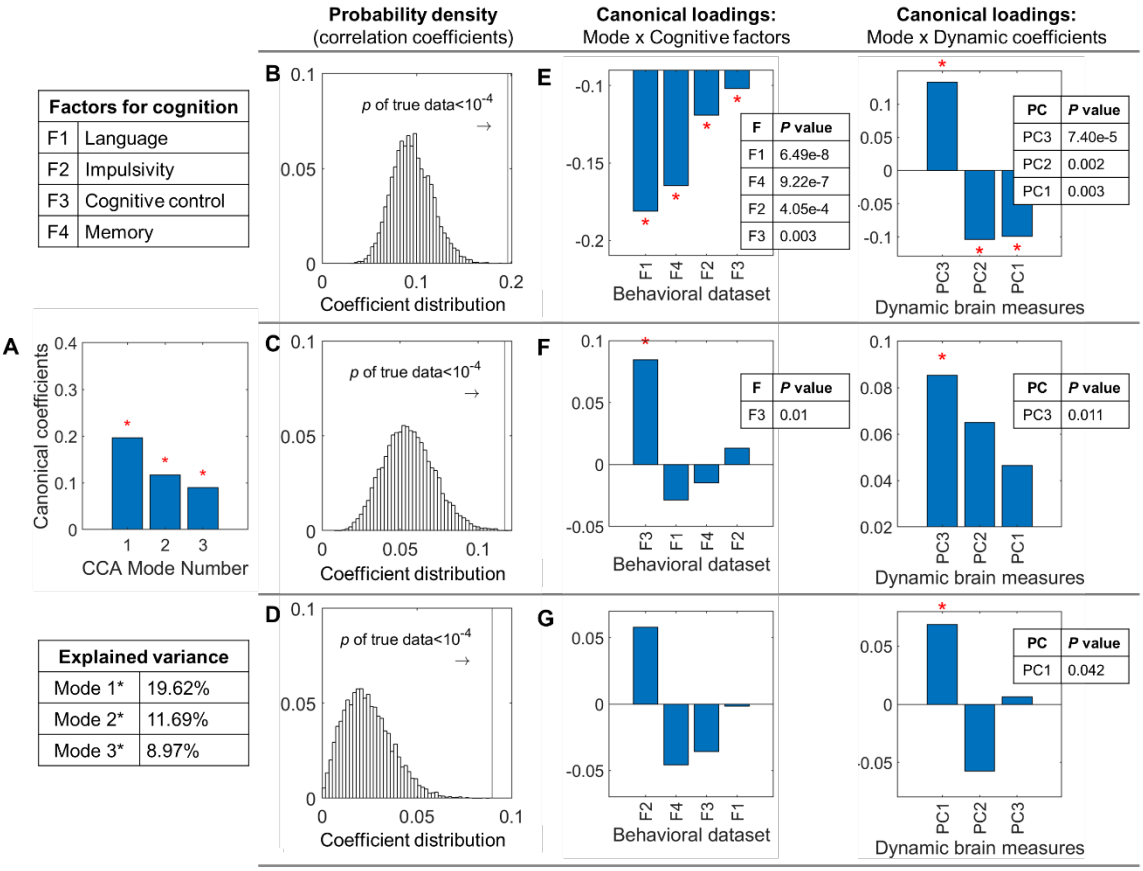

Fig. 4. Dynamic connectome features are related to cognition. (A) Canonical variable X was defined as three principal components, together explaining about 88.51% of the total variance in the temporal phenotypes of the dynamic connectome. Canonical variable Y was defined as four factors, together explaining about 55.10% of the total variance in the cognitive measures. Canonical

correlation analysis (CCA) revealed two significant modes of covariation between these two variables. (B-D) To assess the statistical significance of the discovered modes of covariation, we calculated 10,000 permutations of the rows of X relative to Y, respecting the within-participant structure of the data, and recalculated the CCA mode for each permutation in order to build a distribution of canonical variate pair correlation values (35). By comparing the outcome from the CCA of the true data to the shuffled data, we found that each mode of covariation discovered with the true data was highly significant ($p < 10^{-4}$). (E-G) Post-hoc analysis showed the contribution of the respective variable to each mode. Left panels show the contribution of cognitive factor loadings to each mode, and right panels show the contribution of PC coefficients of connectome dynamics phenotypes to each mode. The X-axis is in ascending order of *p*-value. $P < .05$ was marked with an asterisk. F, factor loading; PC, principal component.

Discussion

Interest in time-varying dynamics of the functional connectome is extensive and fast-growing owing to its potential contribution to cognitive processes and their inter-individual differences. Nevertheless, the growing literature on heritability of connectome features (see below) has largely left out the connectome's inherently multivariate dynamic phenotypes. Because characterization of dynamic connectome reconfigurations involves multiple states, we defined multivariate dynamic phenotypes that wholistically incorporate all states. We show that multivariate dynamic features offer robust evidence of heritability (Fig. 2 and *Fig. S2*), contrasting scalar features (*Fig. S7*), and the cumulative weighted sum of the heritability of scalar features (34) (*Table S2*). Applying this multivariate approach to both temporal and spatial phenotypes, we demonstrate that temporal characteristics of the dynamic functional connectome are indeed heritable. Moreover, we provide the first quantitative heritability estimates and the first potential evidence for genetic effects on dynamic connectome features (Table 1).

Previous studies using classical twin designs have found considerable genetic effects on multiple structural and *static* (i.e., time-averaged) functional connectome features of the human brain. Heritable features of the structural connectome include size (h^2 = 23-60%) and topography (h^2 = 12-19%) of ICNs (36), and average regional controllability as derived from network control theory (h^2 = 13-64%) (37). Regarding the functional connectome, heritability has been established for static FC within canonical neurocognitive ICNs in several studies (h^2 = 13–36% (38); h^2 = 45-80% (5); (h^2 = 9-28% (39)). Further, genetic effects have been reported for topological properties of the static functional connectome, such as global efficiency (h^2 = 52-62%), mean clustering coefficient (h^2 = 47-59%), small-worldness (h^2 = 51-59%), and Modularity (h^2 = 38-59%) (8). Of note, all these structural and functional studies estimated heritability separately for each univariate

connectome feature.

Beyond the above-described studies on structural and static functional connectomes, heritability and quantitative estimation of the genetic impact have been largely unknown for connectome dynamics. A single study has demonstrated heritability of the ratio of time spent across two “metastates”, defined from hierarchical clustering of FO over a 12-state model (12). This finding is exciting in that it establishes the existence of a heritable temporal hierarchy of connectome dynamics. However, this study employed a univariate approach, and the multivariate features of the underlying states were not represented in the heritability assessment. Further, heritability of spatial characteristics of the dynamic states were not studied. Another important, open question is the magnitude of heritability, i.e., % variance of the dynamic features explained by genetic effects.

In this study, we established heritability of multivariate dynamic connectome phenotypes and quantified this influence using structural equation modeling (33). Importantly, we found that heritability of temporal characteristics of state transitions was under substantial genetic influence. Specifically, the additive genetic effect on temporal phenotypes of the dynamic connectome was of high magnitude (h^2 of 35% and of 41% for FO and TP, respectively). This strong heritability is in the range reported above for structural and static FC investigations.

Interestingly, for both FO and TP the effect of common environment was estimated to be zero. To estimate the C factor, twin studies assume that environmental influences are common between MZ and DZ twins, and that the greater phenotypic similarity of MZs must therefore be due to their greater genetic similarity. However, both intrauterine and postnatal environments can differ as a function of zygosity (40). Therefore, the impact of common environment cannot be estimated with precision. Nonetheless, our estimated values suggest that the common environment is unlikely to have a sizeable influence on these phenotypes.

Importantly, we showed that the heritable dynamic features explained inter-individual differences in cognitive abilities. An association with cognition has been previously demonstrated for multiple structural (37) and static functional connectome features (39, 41, 42). A few studies have shown the link between functional connectome dynamics and cognitive measures (11, 12). Consistent with these previous studies and further supporting the potential genetic overlap between connectome dynamics and cognition, our study has demonstrated the association between multivariate temporal dynamic connectome phenotypes and cognitive measures. Crucially, the cognitive measures that we investigated in our study are themselves known to be heritable in the HCP cohort (13). This may suggest that the dynamic connectome features identified in our study are potential endophenotypes for cognitive abilities.

In contrast to the temporal features, we found that heritability was not robustly supported for the spatial features of the dynamic connectome states. Beyond the hypothesis-driven spatial

features ($FC_{DMN\text{-}DAN}$ and Modularity) we tested for the heritability of additional features (i.e., $FC_{DMN\text{-}DAN}$, $FC_{DMN\text{-}CON}$, and data-driven clusters of connections) using ANOVAs and structural equation modelling, and none were consistently significant across methodological choices (See *SI Appendix – Exploring heritability of DMN connectivity to other networks* and *Exploring heritability with network-based statistics*). In principle, this null result may be a false negative due to limited signal-to-noise ratio, limited statistical power, etc. However, the sufficient statistical power for temporal features together with the convergence of outcomes from the ANOVA and component modeling points in the direction of lack of effect for spatial features. We cautiously interpret our data to suggest that genetic effects primarily contribute to how the connectome *transitions* across different states, rather than the precise way in which the states are spatially instantiated in individuals.

Our study is subject to several limitations and methodological considerations. The available sample size is relatively small for a heritability study. This limitation notwithstanding, the confidence intervals demonstrate that the sample size was sufficient to establish the genetic effect on FO and TP with high confidence. Another consideration is that our adaptation of genetic component modeling for multivariate features requires a careful setting of the tangent point. We demonstrated convergence of heritability estimates from the genetics model and the ANOVA approach, which is independent of the tangent point. Thereby, we confirmed that the tangent point of the genetic model was chosen properly.

In conclusion, taking a multivariate approach, our study provides robust converging evidence for a substantial genetic effect on transitions between whole-brain connectome states and the proportion of time spent in each state. Our findings may further indicate that the individually specific instantiation of the states' spatial layout is not heritable. Further, by establishing the association between heritable dynamic connectome features and heritable cognitive traits, this study identifies TP and FO in the resting human brain as potential endophenotypes for cognitive abilities. As such, these features may inform future studies into connectome-based biomarkers of and treatment targets for disorders involving aberrations in the respective cognitive domains.

Materials and Methods

Neuroimaging and Behavior Dataset

We used the Washington University-University of Minnesota (WU-Minn) consortium of the Human Connectome Project (HCP) S1200 release. Participants were recruited, and informed consent was acquired by the WU-Minn HCP consortium according to procedures approved by the Washington University IRB (43). Details of the HCP data collection protocol (44, 45) and cognitive measures (46) are described elsewhere.

From the S1200 HCP data release, following analyses used the data from all 1003 healthy

adult subjects (aged 22-37 y, 534 females) having four complete resting-state fMRI runs (4800 total timepoints). The subjects include 120 monozygotic (MZ) twin pairs, 65 same-sex dizygotic (DZ) twin pairs, 169 non-twin (NT) sibling pairs, and 88 pairs of randomly matched unrelated individuals. Note that all pairs are uniquely defined so that none of the subjects overlap between groups. All 1003 subjects entered HMM estimation of discrete connectome states, while 884 subjects entered heritability so as to avoid dependencies across members of families with > 2 subjects. We included all 14 cognitive measures, which are summary scores for either a cognitive task or a questionnaire, under the cognition domain provided by the HCP (see S1 Table for more detailed description for each variable, and Fig. 1A for their phenotypic correlation structure). The measures were normalized to zero mean and unit variance. Of the selected 884 subjects, 879 subjects had complete data for the 14 cognitive variables measuring cognitive performance.

Neuroimaging Data Preprocessing

All imaging data were acquired on a customized Siemens 3 T Skyra at Washington University in St. Louis using a multi-band sequence. Each 15-minute run of each subject's rfMRI data was preprocessed following the pipeline of Smith et al. (44, 47); it was minimally preprocessed (43) primarily using tools from FSL (48) and Freesurfer (49), and had artifacts removed using ICA+FIX (50, 51). Inter-subject registration of cerebral cortex was carried out using areal-feature-based alignment and the Multimodal Surface Matching algorithm ('MSMAll') (52, 53). For feeding into group-PCA, each dataset was then temporally demeaned and had variance normalization applied (54). We used the preprocessed HCP dataset that retains the global signal (referred to as 'non-GSR data'), and no additional preprocessing was performed. HCP provides averaged BOLD time-series for regions of group-ICA-based parcellations. From the various group-ICA model orders provided by HCP, we chose the highest model order with 300 ICs, which better separates the individual regions of the intrinsic connectivity network (ICN) than the lower-order models. We retained all regions of the cerebrum (139 ICs), excluding the cerebellum and brainstem. These regions were then labeled according to canonical neurocognitive ICNs (55) (*SI Appendix-Parcellations, Fig. S1*).

Hidden Markov modeling

We applied HMM to the above-described minimally preprocessed region-wise BOLD time-series, resulting in K discrete states of whole-brain connectivity patterns and associated state-specific time-courses. The HMM assumes that the time series data can be described using a hidden sequence of a finite number of states. Here, the states represent unique connectivity patterns that repeatedly appear at different time points. Using the HMM-MAR (multivariate autoregressive) toolbox (https://github.com/OHBA-analysis/HMM-MAR), states were inferred from region-wise

BOLD time-series temporally concatenated across all subjects. Whereas the states are estimated at the group level, each subject has a characteristic state time course that indicates the time points at which a given state is active. Following common practice, we ran HMM five times (for a given *K*) over all 1003 subjects to obtain a model that better represents a wider population and selected the run with the best fitting model, i.e., lowest free energy (25, 29, 31).

HMMs require an a priori selection of the number of states, *K*. Generally, the objective is not to establish a 'correct' number of states but to identify a number that describes the dataset at a useful granularity (29). To this end, we chose *Ks* of 4 and 6 based on prior literature. Specificall y, previous HMM literature on brain states has used *K* ranging from 3 to 12 (12, 25–31). We chos e *two* values of *K* within the range of this prior literature, reasoning that robust heritability effects s hould be observable for both. Note that our choice of *K* is also close to the *K* of 5 ~ 7 often identifi ed as optimal in studies using clustering methods as an alternative to HMM (24, 56–58).

Comparison of multivariate features

For each subject and HMM-derived state, we calculated FO (the cumulative total time spent in a given state), $FC_{DMN\text{-}FPN}$ (the mean connectivity across all regions of DMN with those of FPN), and Newman's Modularity (quantifying the level of segregation of each connectome state into modules (32), by applying canonical ICNs (55) as the modular partition and using the greedy algorithm the Brain Connectivity Toolbox (59). Further, we estimated the transition probabilities across all state-pairs (TP matrix) for each subject.

All of these features are multivariate: FO ($1 \times K$), TP matrix ($K \times K$), $FC_{DMN\text{-}FPN}$ ($1 \times K$), and Modularity ($1 \times K$), where *K* denotes the chosen number of discrete connectome states. To investigate whether each of these features is heritable as a multivariate phenotype, we estimated their similarity between subject pairs using Euclidean distance (60). This distance measure preserves the positional relationship between the elements within each multivariate variable. The genetic influence on the Euclidean distance was tested using an ANOVA of the factor sibling status with four levels (i.e., MZ twins, DZ twins, NT siblings, and pairs of unrelated individuals).

Additionally, we examined whether heritability of the features was indeed driven by their multivariate patterns rather than their individual components. Specifically, we individually estimated the similarity of the FO, $FC_{DMN\text{-}FPN}$ and Modularity values of each state, and TP values of each state pair, as their simple difference across subject pairs. These difference values entered a two-way ANOVA of the factors sibling status and connectome states.

Null model

We simulated fifty different new state time courses of the same size as the original

(estimated) state time courses using the *simhmmmar* function provided by HMM-MAR toolbox (https://github.com/OHBA-analysis/HMM-MAR). Note that fifty is a robust number compared to previous work (e.g., Vidaurre et al. (12) applied four simulations). These surrogate datasets preserve the static cross-covariance structure of the original dataset but have randomized state distribution. Then, we ran an HMM inference run with K = 4 and K = 6, respectively, for each surrogate dataset and recomputed the dynamic connectome features at the group- and subject-level, respectively. *Fig. S10* shows that the non-random distributions of features over states observed in the original dataset are absent in the surrogate dataset.

Quantification of heritability

The ACE genetic model is a structural equation model that compares the variance-covariance matrices between MZ and DZ twins. The approach assumes that MZ twins have identical genomes, whereas DZ twins share, on average, half of their genetic information. Assuming that environmental factors influence both types of twins to a similar extent, the variance of a given phenotype can be partitioned into three latent components: additive genetic variance (A), resulting from additive effects of alleles at each contributing locus; shared environmental variance (C), resulting from common environmental effects for both members of a twin pair; and unique environmental variance (E), resulting from nonshared environmental or individual-specific factors (61). Following the parsimony principle, nested models, specifically AE and CE, were fitted by dropping C or A, respectively. Statistical significance of nested models was assessed by a likelihood ratio test, and the fitness of models was tested on the basis of a change in Akaike's Information Criterion (AIC) (62).

We conducted the variance component modeling using *twinlm* in the R package *mets* (http://cran.r-project.org/web/packages/mets/index.html), adjusting for age, sex, and FD (63). As the variance component model finds the relationship between twin pairs, the model requires each subject to have a singular value for each variable. Therefore, the subject-wise phenotypes were obtained by first finding a suitable Euclidean space for a given multivariate feature by taking the mean value of that feature from 50 surrogate datasets (See methods section on *null model*) as the tangent point. For each subject and feature, Euclidean distance from this tangent point was obtained for variance component modeling.

Canonical correlation analysis

Canonical correlation analysis (CCA) finds maximum correlations (or a mode of population covariation) between multidimensional data wherein potential relationships may be present (64). This is a more principled approach compared to conducting all potential correlations and correcting

for multiple comparisons. We used CCA to relate the cognitive measures to phenotypes of the dynamic connectome as previously applied the static connectome (11, 12, 35). We trained CCA on the multivariate variables with reduced dimensionality, including three principal components for dynamic connectome features and four factors for the cognitive measures. We used post-hoc correlations between the modes discovered by the CCA and the cognitive factors to evaluate the contribution of each factor to the given mode. We further assessed the statistical significance of the discovered modes of covariation by performing permutation testing with 10,000 permutations. See *SI Appendix* – *canonical correlation analysis* for details.

Acknowledgments

Data were provided by the Human Connectome Project, WU-Minn Consortium (Principal Investigators: David Van Essen and Kamil Ugurbil; 1U54MH091657) funded by the 16 NIH Institutes and Centers that support the NIH Blueprint for Neuroscience Research; and by the McDonnell Center for Systems Neuroscience at Washington University. We would like to thank Jaime Derringer for her insight and interpretation of quantitative genetic modeling results. AA holds an MRC eMedLab Medical Bioinformatics Career Development Fellowship. This work was partly supported by the Medical Research Council (grant number MR/L016311/1). This work was supported by the National Institute for Mental Health (1R01MH116226 to SS).

References

1. E. S. Finn, *et al.*, Functional connectome fingerprinting: Identifying individuals based on patterns of brain connectivity. *Nat Neurosci* **18**, 1664–1671 (2015).

2. M. Jalbrzikowski, *et al.*, Functional connectome fingerprinting accuracy in youths and adults is similar when examined on the same day and 1.5-years apart. *Hum Brain Mapp* (2020) https:/doi.org/10.1002/hbm.25118.

3. O. T. Ousdal, *et al.*, Longitudinal stability of the brain functional connectome is associated with episodic memory performance in aging. *Hum Brain Mapp* **41**, 697–709 (2020).

4. M. D. Rosenberg, *et al.*, A neuromarker of sustained attention from whole-brain functional connectivity. *Nature Neuroscience* **19**, 165–171 (2016).

5. T. Ge, A. J. Holmes, R. L. Buckner, J. W. Smoller, M. R. Sabuncu, Heritability analysis with repeat measurements and its application to resting-state functional connectivity. *Proc Natl Acad Sci U S A* **114**, 5521–5526 (2017).

6. A. E. Reineberg, A. S. Hatoum, J. K. Hewitt, M. T. Banich, N. P. Friedman, Genetic and Environmental Influence on the Human Functional Connectome. *Cereb. Cortex* **30**, 2099–2113 (2020).

7. W. Liu, N. Kohn, G. Fernández, Intersubject similarity of personality is associated with intersubject similarity of brain connectivity patterns. *Neuroimage* **186**, 56–69 (2019).

8. B. Sinclair, *et al.*, Heritability of the network architecture of intrinsic brain functional connectivity. *Neuroimage* **121**, 243–252 (2015).

9. D. S. Bassett, *et al.*, Dynamic reconfiguration of human brain networks during learning. *Proc. Natl. Acad. Sci. U.S.A.* **108**, 7641–7646 (2011).

10. J. M. Shine, *et al.*, Human cognition involves the dynamic integration of neural activity and neuromodulatory systems. *Nature Neuroscience* **22**, 289–296 (2019).

11. A. Eichenbaum, I. Pappas, D. Lurie, J. R. Cohen, M. D'Esposito, Differential contributions of static and time-varying functional connectivity to human behavior. *Network Neuroscience*, 1–21 (2020).

12. D. Vidaurre, S. M. Smith, M. W. Woolrich, Brain network dynamics are hierarchically organized in time. *Proc. Natl. Acad. Sci. U.S.A.* **114**, 12827–12832 (2017).

13. Y. Han, R. Adolphs, Estimating the heritability of psychological measures in the Human Connectome Project dataset. *PLoS ONE* **15**, e0235860 (2020).

14. S. Sadaghiani, J.-B. Poline, A. Kleinschmidt, M. D'Esposito, Ongoing dynamics in large-scale functional connectivity predict perception. *PNAS* **112**, 8463–8468 (2015).

15. G. J. Thompson, *et al.*, Short-time windows of correlation between large-scale functional brain

networks predict vigilance intraindividually and interindividually. *Human Brain Mapping* **34**, 3280–3298 (2013).

16. L. Douw, D. G. Wakeman, N. Tanaka, H. Liu, S. M. Stufflebeam, State-dependent variability of dynamic functional connectivity between frontoparietal and default networks relates to cognitive flexibility. *Neuroscience* **339**, 12–21 (2016).

17. P. J. Hellyer, *et al.*, The control of global brain dynamics: opposing actions of frontoparietal control and default mode networks on attention. *J Neurosci* **34**, 451–461 (2014).

18. D. Vatansever, A. E. Manktelow, B. J. Sahakian, D. K. Menon, E. A. Stamatakis, Angular default mode network connectivity across working memory load. *Human Brain Mapping* **38**, 41–52 (2017).

19. J. M. Shine, R. A. Poldrack, Principles of dynamic network reconfiguration across diverse brain states. *NeuroImage* **180**, 396–405 (2018).

20. J. R. Cohen, M. D'Esposito, The Segregation and Integration of Distinct Brain Networks and Their Relationship to Cognition. *J. Neurosci.* **36**, 12083–12094 (2016).

21. M. Ekman, J. Derrfuss, M. Tittgemeyer, C. J. Fiebach, Predicting errors from reconfiguration patterns in human brain networks. *PNAS* **109**, 16714–16719 (2012).

22. K. Finc, *et al.*, Transition of the functional brain network related to increasing cognitive demands. *Hum. Brain Mapp.* **3**, e17 (2017).

23. J. M. Shine, *et al.*, The Dynamics of Functional Brain Networks: Integrated Network States during Cognitive Task Performance. *Neuron* **92**, 544–554 (2016).

24. J. S. Nomi, *et al.*, Chronnectomic patterns and neural flexibility underlie executive function. *NeuroImage* **147**, 861–871 (2017).

25. D. Vidaurre, *et al.*, Spectrally resolved fast transient brain states in electrophysiological data. *Neuroimage* **126**, 81–95 (2016).

26. A. P. Baker, *et al.*, Fast transient networks in spontaneous human brain activity. *eLife* **3** (2014).

27. R. Becker, *et al.*, Transient spectral events in resting state MEG predict individual task responses. *NeuroImage* **215**, 116818 (2020).

28. T. Karapanagiotidis, *et al.*, The psychological correlates of distinct neural states occurring during wakeful rest. *Sci Rep* **10**, 21121 (2020).

29. A. J. Quinn, *et al.*, Task-Evoked Dynamic Network Analysis Through Hidden Markov Modeling. *Front Neurosci* **12** (2018).

30. A. B. A. Stevner, *et al.*, Discovery of key whole-brain transitions and dynamics during human wakefulness and non-REM sleep. *Nature Communications* **10**, 1035 (2019).

31. D. Vidaurre, *et al.*, Discovering dynamic brain networks from big data in rest and task. *Neuroimage* **180**, 646–656 (2018).

32. M. E. J. Newman, Finding community structure in networks using the eigenvectors of matrices. *Phys. Rev. E* **74**, 036104 (2006).

33. D. S. Falconer, *Introduction to quantitative genetics.*, 3rd Ed. (Longman Group, 1990).

34. T. Ge, *et al.*, Multidimensional heritability analysis of neuroanatomical shape. *Nat Commun* **7**, 13291 (2016).

35. S. M. Smith, *et al.*, A positive-negative mode of population covariation links brain connectivity, demographics and behavior. *Nature Neuroscience* **18**, 1565–1567 (2015).

36. K. M. Anderson, *et al.*, Heritability of individualized cortical network topography. *PNAS* **118** (2021).

37. W. H. Lee, A. Rodrigue, D. C. Glahn, D. S. Bassett, S. Frangou, Heritability and Cognitive Relevance of Structural Brain Controllability. *Cereb. Cortex* **30**, 3044–3054 (2020).

38. B. M. Adhikari, *et al.*, Comparison of heritability estimates on resting state fMRI connectivity phenotypes using the ENIGMA analysis pipeline. *Hum Brain Mapp* **39**, 4893–4902 (2018).

39. M. L. Elliott, *et al.*, General functional connectivity: Shared features of resting-state and task fMRI drive reliable and heritable individual differences in functional brain networks. *Neuroimage* **189**, 516–532 (2019).

40. D. Conley, E. Rauscher, C. Dawes, P. K. E. Magnusson, M. L. Siegal, Heritability and the Equal Environments Assumption: Evidence from Multiple Samples of Misclassified Twins. *Behav Genet* **43**, 415–426 (2013).

41. M. W. Cole, *et al.*, Multi-task connectivity reveals flexible hubs for adaptive task control. *Nature Neuroscience* **16**, 1348–1355 (2013).

42. M. P. van den Heuvel, O. Sporns, Network hubs in the human brain. *Trends in Cognitive Sciences* **17**, 683–696 (2013).

43. M. F. Glasser, *et al.*, The minimal preprocessing pipelines for the Human Connectome Project. *NeuroImage* **80**, 105–124 (2013).

44. S. M. Smith, *et al.*, Resting-state fMRI in the Human Connectome Project. *Neuroimage* **80**, 144–168 (2013).

45. D. C. Van Essen, *et al.*, The WU-Minn Human Connectome Project: An Overview. *Neuroimage* **80**, 62–79 (2013).

46. D. M. Barch, *et al.*, Function in the human connectome: task-fMRI and individual differences in behavior. *Neuroimage* **80**, 169–189 (2013).

47. S. M. Smith, *et al.*, Functional connectomics from resting-state fMRI. *Trends Cogn. Sci. (Regul. Ed.)* **17**, 666–682 (2013).

48. M. Jenkinson, C. F. Beckmann, T. E. J. Behrens, M. W. Woolrich, S. M. Smith, FSL. *Neuroimage* **62**, 782–790 (2012).

49. B. Fischl, FreeSurfer. *Neuroimage* **62**, 774–781 (2012).

50. L. Griffanti, *et al.*, ICA-based artefact removal and accelerated fMRI acquisition for improved resting state network imaging. *Neuroimage* **95**, 232–247 (2014).

51. G. Salimi-Khorshidi, *et al.*, Automatic denoising of functional MRI data: combining independent component analysis and hierarchical fusion of classifiers. *Neuroimage* **90**, 449–468 (2014).

52. M. F. Glasser, *et al.*, A multi-modal parcellation of human cerebral cortex. *Nature* **536**, 171–178 (2016).

53. E. C. Robinson, *et al.*, MSM: a new flexible framework for Multimodal Surface Matching. *Neuroimage* **100**, 414–426 (2014).

54. C. F. Beckmann, S. M. Smith, Probabilistic independent component analysis for functional magnetic resonance imaging. *IEEE Trans Med Imaging* **23**, 137–152 (2004).

55. B. T. T. Yeo, *et al.*, The organization of the human cerebral cortex estimated by intrinsic functional connectivity. *J. Neurophysiol.* **106**, 1125–1165 (2011).

56. A. Abrol, *et al.*, Replicability of time-varying connectivity patterns in large resting state fMRI samples. *Neuroimage* **163**, 160–176 (2017).

57. E. A. Allen, *et al.*, Tracking whole-brain connectivity dynamics in the resting state. *Cereb. Cortex* **24**, 663–676 (2014).

58. B. Rashid, *et al.*, A framework for linking resting-state chronnectome/genome features in schizophrenia: A pilot study. *Neuroimage* **184**, 843–854 (2019).

59. M. Rubinov, O. Sporns, Complex network measures of brain connectivity: Uses and interpretations. *NeuroImage* **52**, 1059–1069 (2010).

60. G. L. Colclough, *et al.*, The heritability of multi-modal connectivity in human brain activity. *Elife* **6** (2017).

61. A. I. Yashin, I. A. Iachine, Genetic analysis of durations: Correlated frailty model applied to survival of Danish twins. *Genetic Epidemiology* **12**, 529–538 (1995).

62. H. Akaike, Factor analysis and AIC. *Psychometrika* **52**, 317–332 (1987).

63. J. D. Power, K. A. Barnes, A. Z. Snyder, B. L. Schlaggar, S. E. Petersen, Spurious but systematic correlations in functional connectivity MRI networks arise from subject motion. *Neuroimage* **59**, 2142–2154 (2012).

64. H. Hotelling, Relations between two sets of variates. *Biometrika* **28**, 321–377 (1936).

Tables

Table 1. Variance-component model parameter estimates of the dynamic connectome features.

Phenotype	Model	h^2	(95% CI)	A	(95% CI)	C	(95% CI)	E	(95% CI)	-2LL	AIC	χ^2	∆df	p
FO	ACE	.35	(.20, .50)	.35	(20, .50)	.00	(0.0, 0.0)	.65	(.50, .80)	-518.86	-504.86			
	AE	.35	(.19, .50)	.35	(.20, .50)			.65	(.50, .80)	-518.86	-506.86	2.4e-10	1	1.0
	CE					.27	(.14, .41)	.73	(.59, .86)	-516.57	-504.57	2.29	1	.13
TP	ACE	.41	(.27, .55)	.41	(.27,.55)	.00	(0.0, 0.0)	.59	(.45, .73)	-513.43	-499.43			
	AE	.41	(.27, .55)	.41	(.27, .55)			.59	(.45, .73)	-513.43	-501.43	8.1e-12	1	1.0
	CE					.33	(.21, .46)	.67	(.54, .79)	-510.89	-498.89	2.53	1	.11

All models were adjusted for age, sex, and head motion. A, Additive genetic effect; C, common environmental effect; E, Unique/non-shared environment effect; -2LL, twice the negative log-likelihood; AIC, Akaike's information criterion; df, degrees of freedom; χ^2, chi square, ∆df, change in degree of freedom between the full model and the nested model; *p*, χ^2 test in model fitting. The AE and CE models are nested within the ACE model. Each nested model is compared with the fully saturated model. The fitness of models was tested based on a change in AIC (for a change of df of 1, the statistically significant change in χ^2 is 3.84). h^2, the narrow-sense heritability estimated as $\sigma^2_A/(\sigma^2_A + \sigma^2_c + \sigma^2_E)$; CI: Confidence Interval (lower bound, upper bound).